

# High-precision relativistic chiral nucleon-nucleon interaction up to NNLO

Jun-Xu Lu,<sup>1,2</sup> Chun-Xuan Wang,<sup>2</sup> Yang Xiao,<sup>3</sup> Li-Sheng Geng,<sup>2,4,5,\*</sup> Jie Meng,<sup>6</sup> and Peter Ring<sup>7</sup>

<sup>1</sup>*School of Space and Environment, Beihang University, Beijing 102206, China*

<sup>2</sup>*School of Physics, Beihang University, Beijing 102206, China*

<sup>3</sup>*School of Physics, Beihang University, Beijing 102206, China*

<sup>4</sup>*China & Université Paris-Saclay, CNRS/IN2P3, IJCLab, 91405 Orsay, France*

<sup>5</sup>*Beijing Key Laboratory of Advanced Nuclear Materials and Physics, Beihang University, Beijing 102206, China*

<sup>6</sup>*School of Physics and Microelectronics, Zhengzhou University, Zhengzhou, Henan 450001, China*

<sup>7</sup>*State Key Laboratory of Nuclear Physics and Technology, School of Physics, Peking University, Beijing 100871, China*

<sup>7</sup>*Physik Department, Technische Universität München, D-85747 Garching, Germany*

We construct a relativistic chiral nucleon-nucleon interaction up to the next-to-next-to-leading order in covariant baryon chiral perturbation theory. We show that a good description of the  $np$  phase shifts up to  $T_{\text{lab}} = 200$  MeV and even higher can be achieved with a  $\chi^2/\text{d.o.f.}$  less than 1. Both the next-to-leading order results and the next-to-next-to-leading order results describe the phase shifts equally well up to  $T_{\text{lab}} = 200$  MeV, but for higher energies, the latter behaves better, showing satisfactory convergence. The relativistic chiral potential provides the most essential inputs for relativistic ab initio studies of nuclear structure and reactions, which has been in need for almost two decades.

The nucleon-nucleon ( $NN$ ) interaction plays an essential role in our microscopic understanding of nuclear physics. Starting from the pioneering works of Weinberg [1–3], chiral effective field theory (ChEFT) has been successfully applied to derive the  $NN$  interaction. Nowadays the so-called chiral nuclear forces have been constructed up to the fifth order [4–6] and sixth order [7] and reached the level of the most refined phenomenological forces, such as Argonne  $V_{18}$  [8] and CD-Bonn [9], and have become the de facto standard in ab initio nuclear structure and reaction studies [10–13].

Nonetheless, these forces are based on the non-relativistic heavy baryon chiral perturbation theory (ChPT) and cannot be used in relativistic many-body studies [14–18], for which till now only the Bonn potential [19] has been widely used [20]. In addition, there are continuing discussions on the relevance of renormalization group invariance and how the Weinberg power counting should be modified to allow for proper non-perturbative renormalization group invariance [21, 22]. Lorentz covariance, as one of the most fundamental requirements of Nature, may play a role here. It is particularly inspiring to note that in the one-baryon sector covariant baryon ChPT has been shown to provide new perspectives on a number of long standing puzzles, such as baryon magnetic moments [23], Compton scattering off protons [24], pion-nucleon scattering [25], and baryon masses [26, 27].

Recently, a covariant power counting approach similar to the extended-on-mass-shell scheme in the one-baryon sector [28, 29] was proposed to describe the  $NN$  interaction [30, 31]. At leading order (LO), the covariant scheme has been successfully tested in the  $NN$  system [30, 32–35], hyperon-nucleon system [36–41], and  $\Lambda_c N$  system [42, 43]. In addition to providing already a reasonable description of the  $J = 0, 1, 2$   $np$  phase shifts at LO, it also shows some interesting features of proper effective field theories. In Ref. [32], it was shown that for the  $^1S_0$  partial wave, some of the typical low energy features can be reproduced at LO, contrary to the

conventional Weinberg approach. In addition, it also shows improved renormalization group invariance, for example, in the  $^3P_0$  channel [35]. In Ref. [44], it was shown in a hybrid phenomenological approach that the LO relativistic three-body interaction leads to a satisfactory description of polarized  $pd$  scattering data in the whole energy range below the deuteron breakup threshold, solving the longstanding  $A_y$  puzzle thanks to the new terms considered in the  $3N$  force. Furthermore, in Ref. [45], it was shown that the relativistic effects in the perturbative two-pion-exchange (TPE) contributions do improve the description of the peripheral  $NN$  scattering data compared to their non-relativistic counterparts. In Ref. [46], the same feature is found also for the non-perturbative TPE contributions.

It is well known that for realistic studies of nuclear structure and reactions, the covariant chiral force has to be constructed to higher chiral orders.<sup>1</sup> Furthermore, a complete understanding of the covariant chiral nuclear force beyond leading order is also of high relevance. For such purposes, in the present work, we construct the first high precision relativistic  $NN$  interaction up to the next-to-next-to-leading order (NNLO).

In order to take into account the non-perturbative nature of the  $NN$  interaction, we solve the following relativistic Blankenbecler-Sugar (BbS) equation [48],

$$T(\mathbf{p}', \mathbf{p}, s) = V(\mathbf{p}', \mathbf{p}, s) + \int_0^\Lambda \frac{d^3 \mathbf{k}}{(2\pi)^3} V(\mathbf{p}', \mathbf{k}, s) \frac{m^2}{E_k} \frac{1}{q_{cm}^2 - \mathbf{k}^2 - i\epsilon} T(\mathbf{k}, \mathbf{p}, s), \quad (1)$$

where  $|\mathbf{q}_{cm}| = \sqrt{s/4 - m^2}$  is the nucleon momentum on the mass shell in the center of mass (c.m.) frame, and  $\Lambda$  is

<sup>1</sup> Recent studies show that the NNLO non-relativistic chiral forces can provide reliable inputs already, but the N<sup>3</sup>LO forces yield smaller uncertainties [47]

a sharp cutoff to regularize the potential. The momenta of the incoming, outgoing, and intermediate nucleons are depicted in Fig. 1, consistent with the 3D reduction of the Bethe-Salpeter equation to the BbS equation [49].

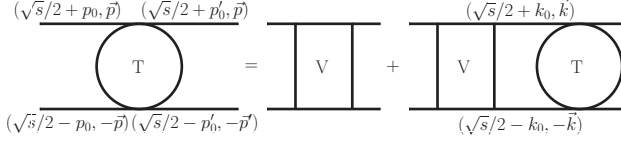


FIG. 1. Kinematics of covariant nucleon-nucleon scattering.

Up to NNLO, the relativistic chiral potential consists of the following terms

$$V = V_{\text{CT}}^{\text{LO}} + V_{\text{CT}}^{\text{NLO}} + V_{\text{OPE}} + V_{\text{TPE}}^{\text{NLO}} + V_{\text{TPE}}^{\text{NNLO}} - V_{\text{IOPE}}, \quad (2)$$

in which the first two terms refer to the LO ( $\mathcal{O}(p^0)$ ) and NLO ( $\mathcal{O}(p^2)$ ) contact contributions, while the next three terms denote the one-pion exchange (OPE), leading, and subleading TPE contributions. The last term represents the iterated OPE contribution.

The chiral effective Lagrangians for the nucleon-nucleon interaction in covariant baryon ChPT have been constructed up to  $\mathcal{O}(p^4)$  in Ref. [31]. There are four contact terms at LO, 13 terms at NLO, and no contact terms at NNLO. As is argued in the Supplementary Material, the large subleading TPE contributions affect the descriptions of some higher partial waves, especially  $^3P_2$ . In order to partially compensate the large subleading TPE contributions to the  $^3P_2$  channel, we promote two nominal  $\text{N}^3\text{LO}$  contact terms to NLO. Considering that in our covariant power counting, the NLO contact terms already contain terms of  $\mathcal{O}(p^4)$  as is depicted in the Supplementary Material, we promote the same terms but originally counted as of  $\text{N}^3\text{LO}$  to NLO for the  $^3P_2$ - $^3F_2$  partial waves. This is equivalent to removing part of the correlations between the higher order contact terms for  $^3P_2$ - $^3F_2$  and the other  $J = 2$  partial waves. Therefore, in the end, we have in total 19 low-energy constants (LECs) up to NNLO. We note that although this number is larger than that of the non-relativistic NNLO potential (9) but smaller than that of  $\text{N}^3\text{LO}$  (24) [50, 51]<sup>2</sup>. In our covariant framework, the 19 LECs contribute to all the partial waves with total angular momentum  $J \leq 2$ , which makes it impossible to reorganize the LECs according to partial waves, different from the non-relativistic cases<sup>3</sup>. We refer to the Supplementary Material for the explicit expressions of the LO and NLO contact potentials.

For the treatment of non-perturbative OPE and TPE contributions, we refer to Ref. [46]. In Table I, we show the values of LECs needed to evaluate the OPE and TPE contributions.

TABLE I. Decay constant  $f_\pi$  (in units of MeV) [11], coupling constant  $g_A$  [11], and NLO  $\pi N$  couplings (in units of  $\text{GeV}^{-1}$ ) [52] adopted for evaluating the OPE and TPE diagrams.

$c_1$	$c_2$	$c_3$	$c_4$	$f_\pi$	$g_A$
-1.39	4.01	-6.61	3.92	92.4	1.29

An important feature of ChEFT is that it allows for reliable uncertainty quantification. In the literature, there are two different ways to estimate the truncation uncertainties of chiral nuclear forces. One is varying the cutoff in a reasonable range, for example, from 450 MeV to 550 MeV [11]. The other is to treat the difference between the optimal results obtained at different orders as the estimate of truncation uncertainties [4]. The latter approach can be briefly described as follows. The expansion parameters for ChEFT read

$$Q = \text{Max}\left\{\frac{p}{\Lambda_b}, \frac{m_\pi}{\Lambda_b}\right\}, \quad (3)$$

where  $p$  is the nucleon momentum in the c.m. frame and  $\Lambda_b$  is the cutoff. One can estimate the NLO and NNLO truncation uncertainties as

$$\begin{aligned} \Delta^{\text{NLO}} &= \text{Max}\{Q^3 \cdot |\delta^{\text{LO}}|, Q \cdot |\delta^{\text{LO}} - \delta^{\text{NLO}}|\}, \\ \Delta^{\text{NNLO}} &= \text{Max}\{Q^4 \cdot |\delta^{\text{LO}}|, Q^2 \cdot |\delta^{\text{LO}} - \delta^{\text{NLO}}|, \\ &\quad Q \cdot |\delta^{\text{NLO}} - \delta^{\text{NNLO}}|\}. \end{aligned} \quad (4)$$

As is shown below, since the optimum cutoff is determined to be 0.6 GeV at NLO but 0.9 GeV at NNLO, we adopt  $\Lambda_b = 0.6$  GeV, which results in more conservative estimates of truncation uncertainties.

In Ref. [46], we showed that the higher partial waves which do not receive contact contributions up to NNLO can be well described with a cutoff of 0.9 GeV. In addition, only the  $^3D_3$  partial wave is sensitive to the cutoff, which implies that higher order LECs are needed for this particular partial wave to achieve renormalization group invariance. As a result, in the fitting of the LECs at NLO and NNLO, we fix the cutoff at 0.9 GeV.

Following the strategy adopted in non-relativistic studies, e.g., Ref. [55], we perform a global fit to the  $np$  phase shifts for all the partial waves with total angular momentum  $J \leq 2$  [54]. For each partial wave, we choose eight data points with laboratory kinetic energy  $T_{\text{lab}} = 1, 5, 10, 25, 50, 100, 150, 200$  MeV for the fitting. The  $\chi^2$ -like function to be minimized,  $\tilde{\chi}^2$ , is defined as

$$\tilde{\chi}^2 = \sum_i (\delta^i - \delta_{\text{PWA93}}^i)^2, \quad (5)$$

where  $\delta^i$  are theoretical phase shifts or mixing angles, and  $\delta_{\text{PWA93}}^i$  are their empirical PWA93 counterparts [54]. A few remarks are in order. First, the  $\tilde{\chi}^2$  defined above does not have proper statistic meaning, as no uncertainties are assigned

<sup>2</sup> It should be noted that the two isospin-violating LECs are not included here. Furthermore, the results of Ref. [51] with which we compare were obtained by setting  $c_{2,3,4}$  semi-free.

<sup>3</sup> Note that in the non-relativistic framework, there is no LEC for the  $^3F_2$  partial wave up to  $\text{N}^3\text{LO}$ .

TABLE II. LECs (in units of  $10^4 \text{GeV}^{-2}$ ) for the covariant LO, NLO, and NNLO results shown in Fig. 2.

	$O_1$	$O_2$	$O_3$	$O_4$	$O_5$	$O_6$	$O_7$	$O_8$	$O_9$	$O_{10}$	$O_{11}$	$O_{12}$	$O_{13}$	$O_{14}$	$O_{15}$	$O_{16}$	$O_{17}$	$D_1$	$D_2$
LO	-13.23	-2.06	-9.34	3.14															
NLO	-2.62	9.45	-5.42	-6.05	30.09	9.02	-9.19	8.74	4.74	7.02	3.52	11.42	-6.03	-20.55	-4.99	-12.80	6.30	0.42	0.28
NNLO	-14.83	-2.25	-4.85	6.24	-0.82	1.96	-6.89	7.19	1.44	3.50	-8.10	-9.38	-4.33	-12.89	-12.26	-11.69	3.86	-1.88	-0.63

TABLE III.  $\tilde{\chi}^2 = \sum_i (\delta^i - \delta_{\text{PWA93}}^i)^2$  of different chiral forces for partial waves up to  $J \leq 2$ .

	Total	$^1S_0$	$^3P_0$	$^1P_1$	$^3P_1$	$^3S_1$	$^3D_1$	$\epsilon_1$	$^1D_2$	$^3D_2$	$^3P_2$	$^3F_2$	$\epsilon_2$
NLO	17.02	1.02	7.04	0.46	0.33	1.80	1.69	0.15	2.18	1.35	0.95	0.01	0.04
NNLO	16.61	0.18	0.30	1.07	1.55	3.36	0.26	0.03	0.01	9.56	0.01	0.27	0.01
NR-N <sup>3</sup> LO-DR	8.84	1.53	0.30	2.41	0.04	2.33	1.00	0.02	0.57	0.42	0.17	0.03	0.02
NR-N <sup>3</sup> LO-SFR	16.08	13.45	0.29	0.34	0.06	0.01	0.13	0.01	0.02	0.43	0.12	1.22	0.00

and the number of data fitted is a bit arbitrary (eight for each partial wave in the present study). Second, as the same uncertainties for the phase shifts and mixing angle are assumed, this necessarily put more weights on those partial waves of large magnitude, for example,  $^1S_0$  and  $^3S_1$ .

The so-obtained fitting results are shown in Fig. 2, where the theoretical uncertainties are generated following Eq. (4). The corresponding LECs are given in Table II. For comparison, we also show the non-relativistic N<sup>3</sup>LO results obtained with either dimensional regularization (NR-N<sup>3</sup>LO-DR) [11, 51] or spectral-function regularization (NR-N<sup>3</sup>LO-SFR) [53].

First we notice that the NLO and NNLO covariant results describe the  $np$  phase shifts very well up to  $T_{\text{lab}} = 200$  MeV, at a level similar to the non-relativistic N<sup>3</sup>LO results. Particularly interesting is that the NLO and the NNLO results also agree well with each other for  $T_{\text{lab}} \leq 200$  MeV, while the NNLO results are in better agreement the PWA data for larger kinetic energies. This demonstrates that the chiral series converge well. On the other hand, for  $^3F_2$ , the NLO results are better, which can be attributed to the compromise that one has to make to fit all the  $J = 2$  partial waves with five LECs to balance the large contributions of subleading TPE. It can be largely improved once the correlation between the  $D$ -waves with  $J = 2$  and  $^3P_2$ - $^3F_2$  are removed, i.e., the  $D$ -waves and  $^3P_2$ - $^3F_2$  are fitted separately or the cutoff is slightly modified. We note that in obtaining the NR-N<sup>3</sup>LO-DR results, the phase shifts of this channel were lowered by a careful fine-tuning of  $c_2$  and  $c_4$  [51].

The  $\tilde{\chi}^2$ 's for each partial wave are given in Table IV. Judging from the total  $\tilde{\chi}^2$ , the quality of the covariant fits is compatible to the N<sup>3</sup>LO results obtained with either the dimensional regularization or the spectral-function regularization. Comparing the NR-N<sup>3</sup>LO-SFR results with the covariant NNLO results, we find that although the total  $\tilde{\chi}^2$ 's are similar, they originate from different partial waves. The largest contribution to the total  $\tilde{\chi}^2$  of NR-N<sup>3</sup>LO-SFR comes from the  $^1S_0$  partial wave while that of our NNLO results originates from the  $^3D_2$  partial wave. It should also be noted that if we

set the cutoff at 0.8 GeV, we can achieve a total  $\tilde{\chi}^2$  as small as 5.3 (see the Supplementary Material for details), which is even smaller than that of NR-N<sup>3</sup>LO-DR, which is about 9. However, as shown in Ref. [46], the  $^3D_3$  partial wave cannot be well described with a cutoff of 0.8 GeV. Therefore, in the present work, we stick to the cutoff of 0.9 GeV.

To summarize, we constructed a relativistic chiral nucleon-nucleon interaction up to the next-to-next-to-leading order in covariant baryon chiral perturbation theory. The 19 low energy constants were fixed by fitting to all the partial wave phase shifts with total angular momentum  $J \leq 2$ . We obtained a quite good description of the PWA93 phase shifts. The next-to-leading order and the next-to-next-to-leading order results agree well with each other for  $T_{\text{lab}} \leq 200$  MeV, while at higher energies the NNLO results agree better with the PWA93 phase shifts. This demonstrated the convergence of the covariant chiral expansions. Given the quality already achieved in describing the  $np$  phase shifts, the NNLO covariant chiral  $NN$  interaction provides the much wanted inputs for relativistic ab initio nuclear structure and reaction studies. In particular, it may provide new insights into many long-standing problems, e.g., the  $A_y$  puzzle, in combination with the leading order covariant  $3N$  chiral force explored in Ref. [44], which appears at NNLO.

This work is supported in part by the National Natural Science Foundation of China under Grants No.11735003, No.11975041, and No.11961141004. Jun-Xu Lu acknowledges support from the National Natural Science Foundation of China under Grants No.1210050991. Jie Meng acknowledges support from the National Science Foundation of China (NSFC) under Grants No. 11935003 and the National Key R & D Program of China (Contracts No. 2017YFE0116700). Peter Ring acknowledges partial support from the Deutsche Forschungsgemeinschaft (DFG, German Research Foundation) under Germany's Excellence Strategy—EXC-2094—390783311.

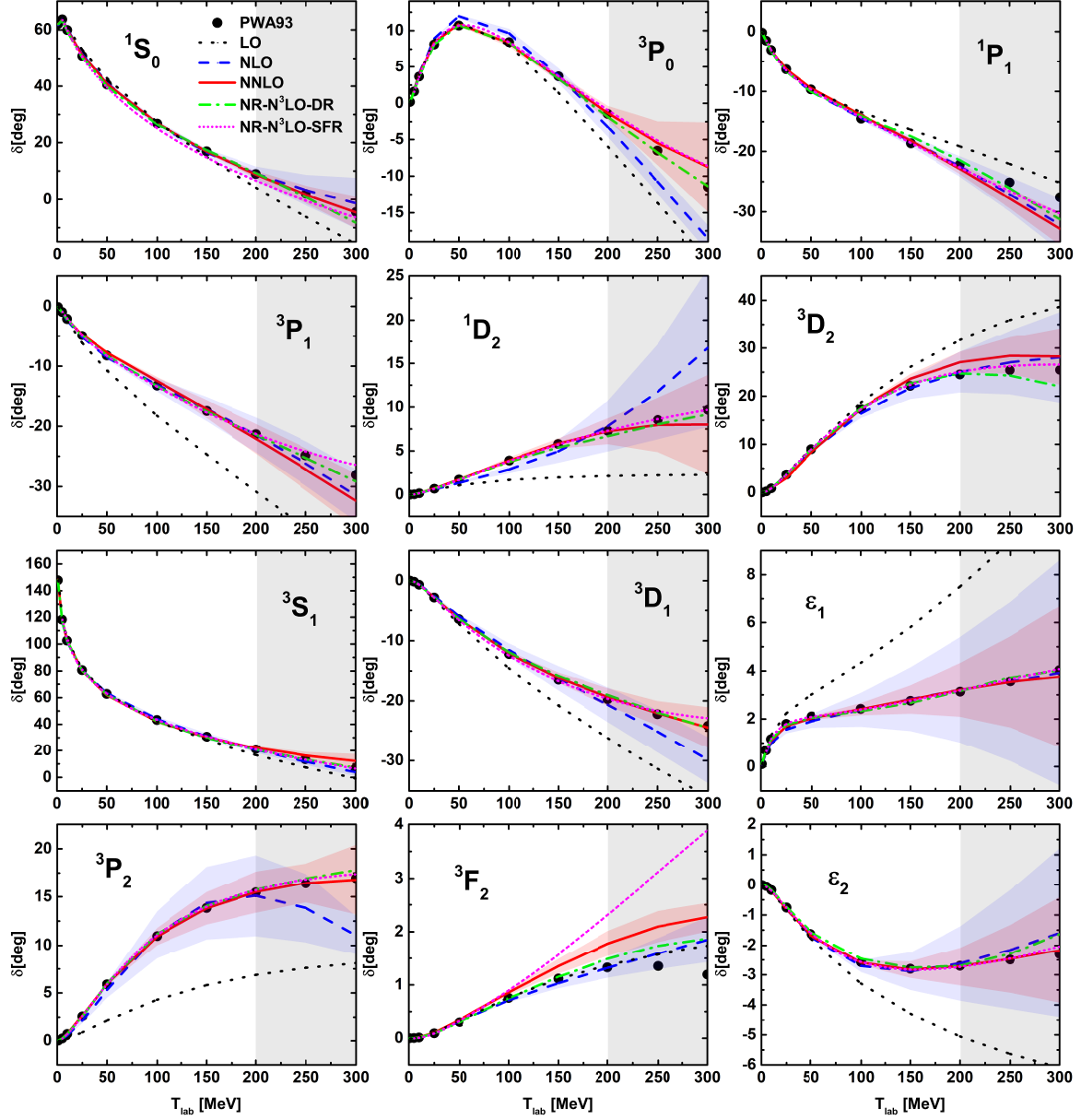


FIG. 2.  $NN$  phase shifts for partial waves with  $J \leq 2$ . The red solid lines denote the covariant NNLO results obtained with a cutoff of  $\Lambda = 0.9$  GeV and the blue dashed lines denote the NLO covariant results obtained with a smaller cutoff of  $\Lambda = 0.6$  GeV. For comparison, we also show the LO covariant results (black dotted lines) obtained with a cutoff of  $\Lambda = 0.6$  GeV and the non-relativistic  $N^3\text{LO}$  results obtained with dimensional regularization (NR- $N^3\text{LO-DR}$ ,  $\Lambda = 0.5$  GeV, green dash-dotted lines) [11, 51] and with spectral-function regularization [53] (NR- $N^3\text{LO-SFR}$ , cutoff = 0.9 fm, magenta short-dotted lines). The black dots denote the PWA93 phase shifts [54]. The shaded regions denote that those data are not fitted and the corresponding covariant results are predictions.

\* Email: lisheng.geng@buaa.edu.cn

- [1] S. Weinberg, Phys. Lett. **B251**, 288 (1990).
- [2] S. Weinberg, Nucl. Phys. **B363**, 3 (1991).
- [3] S. Weinberg, Phys. Lett. B **295**, 114 (1992), arXiv:hep-ph/9209257.
- [4] E. Epelbaum, H. Krebs, and U.-G. Meißner,

Phys. Rev. Lett. **115**, 122301 (2015).

- [5] P. Reinert, H. Krebs, and E. Epelbaum, Eur. Phys. J. A **54**, 86 (2018), arXiv:1711.08821 [nucl-th].
- [6] D. R. Entem, R. Machleidt, and Y. Nosyk, Phys. Rev. **C96**, 024004 (2017).
- [7] D. Rodriguez Entem, R. Machleidt, and Y. Nosyk, Front. in Phys. **8**, 57 (2020).
- [8] R. B. Wiringa, V. G. J. Stoks, and R. Schiavilla, Phys. Rev. **C51**, 38 (1995).



- [9] R. Machleidt, Phys. Rev. **C63**, 024001 (2001).
- [10] E. Epelbaum, H.-W. Hammer, and U.-G. Meißner, Rev. Mod. Phys. **81**, 1773 (2009).
- [11] R. Machleidt and D. R. Entem, Phys. Rept. **503**, 1 (2011).
- [12] H. W. Hammer, S. König, and U. van Kolck, Rev. Mod. Phys. **92**, 025004 (2020), arXiv:1906.12122 [nucl-th].
- [13] C. Drischler, W. Haxton, K. McElvain, E. Mereghetti, A. Nicholson, P. Vranas, and A. Walker-Loud, Prog. Part. Nucl. Phys. **121**, 103888 (2021), arXiv:1910.07961 [nucl-th].
- [14] S. Shen, J. Hu, H. Liang, J. Meng, P. Ring, and S. Zhang, Chin. Phys. Lett. **33**, 102103 (2016).
- [15] S. Shen, H. Liang, J. Meng, P. Ring, and S. Zhang, Phys. Rev. C **96**, 014316 (2017), arXiv:1705.01691 [nucl-th].
- [16] H. Tong, X.-L. Ren, P. Ring, S.-H. Shen, S.-B. Wang, and J. Meng, Phys. Rev. C **98**, 054302 (2018), arXiv:1808.09138 [nucl-th].
- [17] H. Tong, P.-W. Zhao, and J. Meng, Phys. Rev. C **101**, 035802 (2020), arXiv:1903.05938 [nucl-th].
- [18] S. Wang, Q. Zhao, P. Ring, and J. Meng, Phys. Rev. C **103**, 054319 (2021), arXiv:2103.12960 [nucl-th].
- [19] R. Machleidt, K. Holinde, and C. Elster, Phys. Rept. **149**, 1 (1987).
- [20] S. Shen, H. Liang, W. H. Long, J. Meng, and P. Ring, Prog. Part. Nucl. Phys. **109**, 103713 (2019), arXiv:1904.04977 [nucl-th].
- [21] E. Epelbaum, A. M. Gasparyan, J. Gegelia, and U.-G. Meißner, Eur. Phys. J. A **54**, 186 (2018), arXiv:1810.02646 [nucl-th].
- [22] U. van Kolck, Front. in Phys. **8**, 79 (2020), arXiv:2003.06721 [nucl-th].
- [23] L. S. Geng, J. Martin Camalich, L. Alvarez-Ruso, and M. J. Vicente Vacas, Phys. Rev. Lett. **101**, 222002 (2008), arXiv:0805.1419 [hep-ph].
- [24] V. Lensky and V. Pascalutsa, Eur. Phys. J. C **65**, 195 (2010), arXiv:0907.0451 [hep-ph].
- [25] J. M. Alarcon, J. Martin Camalich, and J. A. Oller, Phys. Rev. D **85**, 051503 (2012), arXiv:1110.3797 [hep-ph].
- [26] J. Martin Camalich, L. S. Geng, and M. J. Vicente Vacas, Phys. Rev. D **82**, 074504 (2010), arXiv:1003.1929 [hep-lat].
- [27] X.-L. Ren, L.-S. Geng, J. Martin Camalich, J. Meng, and H. Toki, JHEP **12**, 073 (2012).
- [28] J. Gegelia and G. Japaridze, Phys. Rev. D **60**, 114038 (1999), arXiv:hep-ph/9908377.
- [29] T. Fuchs, J. Gegelia, G. Japaridze, and S. Scherer, Phys. Rev. D **68**, 056005 (2003), arXiv:hep-ph/0302117.
- [30] X.-L. Ren, K.-W. Li, L.-S. Geng, B.-W. Long, P. Ring, and J. Meng, Chin. Phys. C **42**, 014103 (2018).
- [31] Y. Xiao, L.-S. Geng, and X.-L. Ren, Phys. Rev. C **99**, 024004 (2019), arXiv:1812.03005 [nucl-th].
- [32] X.-L. Ren, C.-X. Wang, K.-W. Li, L.-S. Geng, and J. Meng, Chin. Phys. Lett. **38**, 062101 (2021), arXiv:1712.10083 [nucl-th].
- [33] Q.-Q. Bai, C.-X. Wang, Y. Xiao, and L.-S. Geng, Phys. Lett. **B**, 135745 (2020), arXiv:2007.01638 [nucl-th].
- [34] Q.-Q. Bai, C.-X. Wang, Y. Xiao, and L.-S. Geng, (2021), arXiv:2105.06113 [hep-ph].
- [35] C.-X. Wang, L.-S. Geng, and B. Long, Chin. Phys. C **45**, 054101 (2021), arXiv:2001.08483 [nucl-th].
- [36] K.-W. Li, X.-L. Ren, L.-S. Geng, and B. Long, Phys. Rev. **D94**, 014029 (2016).
- [37] K.-W. Li, X.-L. Ren, L.-S. Geng, and B.-W. Long, Chin. Phys. C **42**, 014105 (2018), arXiv:1612.08482 [nucl-th].
- [38] K.-W. Li, T. Hyodo, and L.-S. Geng, Phys. Rev. C **98**, 065203 (2018), arXiv:1809.03199 [nucl-th].
- [39] J. Song, K.-W. Li, and L.-S. Geng, Phys. Rev. C **97**, 065201 (2018), arXiv:1802.04433 [nucl-th].
- [40] Z.-W. Liu, J. Song, K.-W. Li, and L.-S. Geng, Phys. Rev. C **103**, 025201 (2021), arXiv:2011.05510 [nucl-th].
- [41] J. Song, Z.-W. Liu, K.-W. Li, and L.-S. Geng, (2021), arXiv:2107.04742 [nucl-th].
- [42] J. Song, Y. Xiao, Z.-W. Liu, C.-X. Wang, K.-W. Li, and L.-S. Geng, Phys. Rev. C **102**, 065208 (2020), arXiv:2010.06916 [nucl-th].
- [43] J. Song, Y. Xiao, Z.-W. Liu, K.-W. Li, and L.-S. Geng, (2021), arXiv:2104.02380 [hep-ph].
- [44] L. Giralda, A. Kievsky, M. Viviani, and L. E. Marcucci, Phys. Rev. C **99**, 054003 (2019), arXiv:1811.09398 [nucl-th].
- [45] Y. Xiao, C.-X. Wang, J.-X. Lu, and L.-S. Geng, Phys. Rev. C **102**, 054001 (2020), arXiv:2007.13675 [nucl-th].
- [46] C.-X. Wang, J.-X. Lu, Y. Xiao, and L.-S. Geng, (2021), arXiv:2110.05278 [nucl-th].
- [47] T. H  ther, K. Vobig, K. Hebeler, R. Machleidt, and R. Roth, Phys. Lett. B **808**, 135651 (2020), arXiv:1911.04955 [nucl-th].
- [48] R. Blankenbecler and R. Sugar, Phys. Rev. **142**, 1051 (1966).
- [49] R. M. Woloshyn and A. D. Jackson, Nucl. Phys. B **64**, 269 (1973).
- [50] E. Epelbaum, W. Glockle, and U.-G. Meißner, Nucl. Phys. **A747**, 362 (2005).
- [51] D. R. Entem and R. Machleidt, Phys. Rev. **C68**, 041001 (2003).
- [52] Y.-H. Chen, D.-L. Yao, and H. Q. Zheng, Phys. Rev. D **87**, 054019 (2013), arXiv:1212.1893 [hep-ph].
- [53] E. Epelbaum, H. Krebs, and U. G. Meißner, Eur. Phys. J. **A51**, 53 (2015).
- [54] V. G. J. Stoks, R. A. M. Klomp, M. C. M. Rentmeester, and J. J. de Swart, Phys. Rev. **C48**, 792 (1993).
- [55] E. Epelbaum, W. Gloeckle, and U.-G. Meißner, Nucl. Phys. **A671**, 295 (2000).
- [56] E. Epelbaum, W. Gloeckle, and U.-G. Meissner, Eur. Phys. J. A **19**, 125 (2004), arXiv:nucl-th/0304037.
- [57] E. Epelbaum, W. Gloeckle, and U.-G. Meissner, Eur. Phys. J. A **19**, 401 (2004), arXiv:nucl-th/0308010.

## Supplementary Material for “High-precision relativistic chiral nucleon-nucleon interaction up to NNLO”

In this supplemental material, we provide further details that are useful to understand the results presented in the main text.

### FITS WITH 17 LECs

In this section, we present the  $NN$  scattering phase shifts obtained in our NNLO chiral nuclear force with 17 LECs as dictated in Ref. [31], and explain why two nominal N<sup>3</sup>LO contact terms need to be promoted.

Following the same fitting strategy as detailed in the main text, we obtain the results shown in Fig. 3, which are denoted by “CO-NNLO” to distinguish it from the “NNLO” results presented in the main text. For comparison, we also show the non-relativistic NNLO and N<sup>3</sup>LO results obtained with the dimensional regularization and spectral-function regularization, which are referred to as “NR-NNLO-DR” [55], “NR-N<sup>3</sup>LO-DR” [51], and “NR-N<sup>3</sup>LO-SFR” [4], respectively. In Table. IV, we tabulate the  $\chi^2$  obtained by fitting to the PWA93 phase shifts at laboratory energies  $T_{\text{lab}} = 1, 5, 10, 25, 50, 100, 150, 200$  MeV for each partial wave, as well as the sum of them. Clearly, compared to the results shown in the main text, only the  $^3P_2$  partial wave cannot be satisfactorily described.

It was already noticed in Ref. [55] that the non-relativistic subleading TPE potential is a bit strong such that the description of the phase shifts can be worsened at NNLO for some partial waves, e.g., the  $^3P_2$  partial wave. This was attributed to the dimensional regularization applied in regularizing the TPE loop diagrams that takes into account the high-momentum contribution of pion loops. Replacing the dimensional regularization with the so-called spectrum functional regularization, which is essentially a cutoff regularization, improves the description of  $^3P_2$  at NNLO (but worsens the description of some other partial waves [50, 53, 56, 57]). On the other hand, a better description with the dimensional regularization can be obtained when the non-relativistic chiral potential was constructed up to N<sup>3</sup>LO [51], which yields results in good agreement with the PWA93 phase shifts for all the partial waves considered there (but with a dedicate fine-tuning of the NLO LECs  $c_2$  and  $c_4$ ). In addition, since there is no LEC to balance the large TPE contributions except the cutoff and the NLO LECs of  $\pi N$  scattering  $c_1, c_2, c_3, c_4$ ,  $V_{\text{TPE}}^{\text{NNLO}}$  introduces strong cutoff dependence for the partial waves with orbital angular momentum  $L = 2$ , particularly,  $^3D_3$ . This problem can be alleviated after the non-relativistic chiral potential is constructed up to N<sup>3</sup>LO in which new LECs are introduced.

In our study, we find that the relativistic potential also suffers from the two problems mentioned above but to a less extent. The contributions from the relativistic  $V_{\text{TPE}}^{\text{NNLO}}$  is large and compatible with (but smaller than) their corresponding non-relativistic counterparts [45].

The large subleading TPE contributions force the  $^3P_2$  phase shifts to drop down with increasing  $T_{\text{lab}}$ . To compensate them, we promote two of the higher order contact terms to NLO for the  $^3P_2$ - $^3F_2$  coupled channel, which is equivalent to break the correlations between the  $J = 2$  partial waves. In the following we explain in detail how we achieved this.

In our covariant power counting scheme [31], the NLO contact terms for the  $J = 2$  partial waves already contain nominally higher order contact terms (in the language of HBChPT) as is explicitly exhibited in Eq. (20). Obviously, for the two  $D$ -waves, at this order, the contact terms are counted nominally as of  $\mathcal{O}(p^4)$ . For  $^3P_2$ , the first term is counted as of order  $\mathcal{O}(p^2)$ , while the other two terms are of order  $\mathcal{O}(p^4)$  and  $\mathcal{O}(p^6)$ , respectively. The situation is similar for  $^3F_2$  and the off-diagonal  $^3P_2$ - $^3F_2$ . This way, we have in total eight different structures, corresponding to eight combinations of the NLO LECs ( $O_{5,\dots,17}$ ) for all the  $J = 2$  partial waves, while only three of them are independent.

On the other hand, at N<sup>3</sup>LO, the contact terms contain the same structures of nominal order  $\mathcal{O}(p^4)$  for these partial waves. The only difference is that at N<sup>3</sup>LO, the coefficients for these terms are composed of the N<sup>3</sup>LO LECs ( $O_{18,\dots,40}$ ) [31]. The relevant terms of order  $\mathcal{O}(p^4)$  for  $^3P_2$  and  $^3P_2$ - $^3F_2$  at N<sup>3</sup>LO read

$$\begin{aligned} V_{3P_2}^{N^3LO} &= D_1 \frac{\pi p p' (\Delta_p + \Delta_{p'})}{m^3}, \\ V_{3P_2-3F_2}^{N^3LO} &= D_2 \frac{\pi p p'^3}{m^3 N_{p'}}, \end{aligned} \quad (6)$$

in which  $\Delta_p, \Delta_{p'}, N_{p'}$  are defined in Eq. (9). The  $D_1$  and  $D_2$  are

$$\begin{aligned} D_1 &= (-2O_{18} - O_{19} - O_{20} - 10O_{21} - 9O_{22} - 10O_{24} \\ &\quad - 10O_{25} + 10O_{26} - 20O_{27} - 2O_{28} - O_{29} - O_{30} \\ &\quad - 10O_{31} - 9O_{32} - 10O_{33} - 12O_{34} + 12O_{35} - 16O_{36} \\ &\quad - 10O_{37} - 14O_{38} + 14O_{39} - 12O_{40})/30, \\ D_2 &= -5\sqrt{\frac{3}{2}}(2O_{18} + O_{19} + O_{20} - O_{22} + 2O_{28} \\ &\quad + O_{29} + O_{30} - O_{32} + 2O_{34} - 2O_{35} - 4O_{36} + 4O_{38} \\ &\quad - 4O_{39} - 8O_{40}). \end{aligned} \quad (7)$$

In the present work, we promote these two additional terms of Eq. (6) from N<sup>3</sup>LO to  $V_{3P_2}^{NLO}$  and  $V_{3P_2-3F_2}^{NLO}$  in Eq. (20). This is equivalent to performing the following replacements,

$$C_2^{3P_2} \rightarrow C_2^{3P_2} + D_1, \quad C_1^{3PF_2} \rightarrow C_1^{3PF_2} + D_2. \quad (8)$$

This way, we break the correlation between  $C_2^{3P_2}$ ,  $C_1^{3PF_2}$ , and the other six combinations. We have now five independent combinations of LECs for the  $J = 2$  partial waves instead of three. We have checked that the two combinations  $D_1$  and  $D_2$  only contribute to the  $^3P_2$  and  $^3P_2$ - $^3F_2$  partial waves, which leads to a much better description of the  $^3P_2$  partial wave. Therefore, in total, we have 19 LECs for the NNLO potential presented in the main text.

TABLE IV.  $\chi^2 = \sum_i (\delta^i - \delta_{\text{PWA93}}^i)^2$  of different chiral forces of partial waves up to  $J \leq 2$ .

	Total	$^1S_0$	$^3P_0$	$^1P_1$	$^3P_1$	$^3S_1$	$^3D_1$	$\epsilon_1$	$^1D_2$	$^3D_2$	$^3P_2$	$^3F_2$	$\epsilon_2$
CO-NNLO	51.64	0.29	0.29	1.13	1.50	3.40	0.01	0.15	0.01	9.71	34.73	0.41	0.03
NR-NNLO	289.59	2.68	27.49	2.32	20.96	0.62	0.25	1.55	0.06	12.47	217.42	2.52	1.26
NR-N <sup>3</sup> LO-DR	8.84	1.53	0.30	2.41	0.04	2.33	1.00	0.02	0.57	0.42	0.17	0.03	0.02
NR-N <sup>3</sup> LO-SFR	16.08	13.45	0.29	0.34	0.06	0.01	0.13	0.01	0.02	0.43	0.12	1.22	0.00

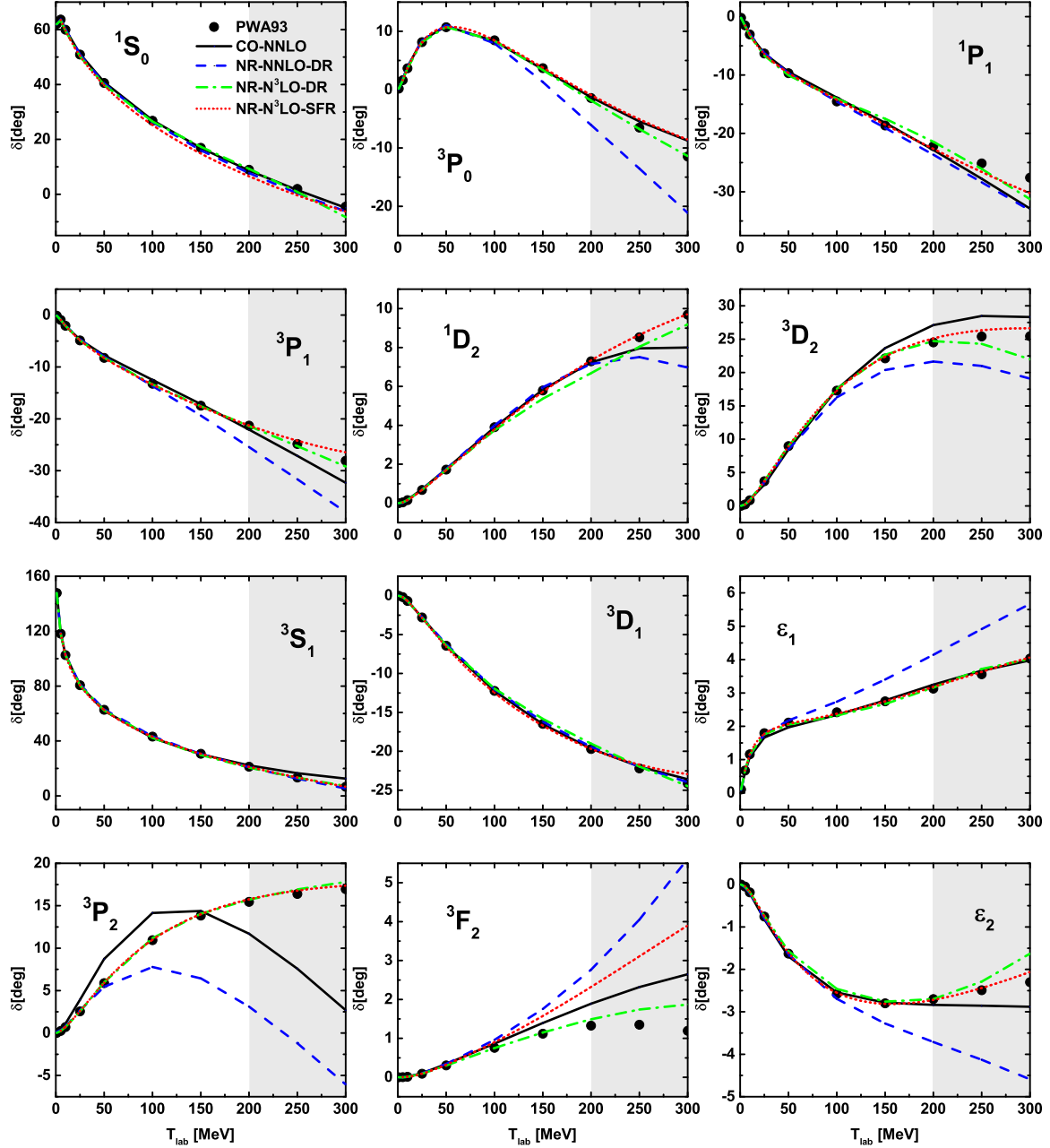


FIG. 3.  $NN$  phase shifts for the partial waves with total angular momentum  $J \leq 2$ . The black solid line denotes the CO-NNLO results obtained with a cutoff  $\Lambda = 0.9$  GeV. For comparison, we also show the non-relativistic results obtained with the dimensional regularization up to NNLO (NR-NNLO-DR,  $\Lambda = 0.875$  GeV, blue dashed lines) [55] and N<sup>3</sup>LO (NR-N<sup>3</sup>LO-DR,  $\Lambda = 0.5$  GeV, green dash-dotted lines) [51], as well as the non-relativistic N<sup>3</sup>LO results with spectral-function regularization (NR-N<sup>3</sup>LO-SFR,  $\Lambda = 0.9$  fm, red dotted lines). The black dots denote the empirical PWA93 phase shifts [54]. The shadows represent the energy region not taken into account in the fitting.

## INFLUENCE OF CUTOFF VARIATIONS FROM 0.8 GEV TO 0.9 GEV

In Fig. 4, we compare the covariant NNLO fits obtained with a cutoff of 0.9 GeV and 19 LECs and those obtained with a smaller cutoff of 0.8 GeV. With the cutoff switched to 0.8 GeV, we obtain a relatively better description of  $^3P_0$ ,  $^3D_2$ , and  $^3F_2$  for  $T_{\text{lab}} \leq 200$  MeV and thus a much smaller  $\tilde{\chi}^2 \sim 5.29$ . Clearly, the cutoff dependence is visible only for the  $^3F_2$ ,  $^3D_2$  phase shifts and the mixing angle  $\epsilon_2$  at higher kinetic energies. This indicates that for these partial waves, inclusion of higher chiral order contributions is necessary.

For the  $^3D_3$  partial wave to which no contact term contributes, the phase shifts are more sensitive to the choice of the cutoff as is shown in Fig. 5. This is the main reason why we stick to the cutoff of 0.9 GeV. However, we find that once the N<sup>3</sup>LO contact terms are introduced, the cutoff dependence can be largely suppressed.

### COMPARISON WITH THE NR-N<sup>3</sup>LO-DR RESULTS FOR HIGHER PARTIAL WAVES

In Fig. 5, we compare the NR-N<sup>3</sup>LO-DR chiral force [11, 51] with the covariant NNLO chiral force for peripheral partial waves with  $J \leq 4$  and  $L \leq 4$ . Higher partial waves are not explicitly shown since for them the OPE plays the dominated role.

The  $\tilde{\chi}^2$  for each partial wave are collected in Table V. Clearly for these partial waves, the covariant NNLO results are as good as or even slightly better than the NR-N<sup>3</sup>LO-DR results for  $T_{\text{lab}} \leq 200$  MeV except for  $^3F_3$  and  $^3F_4$ . For  $^3D_3$  and  $^1F_3$ , our covariant NNLO results are not able to describe well the high-momentum data, while the NR-N<sup>3</sup>LO-DR results miss the data for  $T_{\text{lab}} \in [100, 200]$  MeV. For  $^3F_3$ , no results can reproduce the behavior above  $T_{\text{lab}} = 200$  MeV but the NR-N<sup>3</sup>LO-DR results are slightly better. The large part of the  $\tilde{\chi}^2$  for our covariant NNLO results comes from  $^3F_4$ , in which the subleading TPE is strong such that it shifts the results well above the PWA93 phase shifts, while the NR-N<sup>3</sup>LO-DR results behave much better. For the  $G$ -waves and the mixing angle  $\epsilon_3$ , both results are in pretty good agreement with the empirical data below  $T_{\text{lab}} = 200$  MeV, while the NR-N<sup>3</sup>LO-DR results tend to yield smaller values at higher energies.

### COMPARISON WITH THE BONN POTENTIAL

For years, in relativistic studies of nuclear structure and reactions, the Bonn potential developed in the 1980's has been the only choice [20]. In Figs. 6 and 7, we compare the phase shifts for partial wave with  $J \leq 7$ . It is clear that on average the covariant chiral nuclear force provides a better description of the PWA93 phase shifts than the Bonn potential, for example,  $^1S_0$ ,  $^3P_0$ ,  $^3D_1$ , and  $^3D_3$ .

## CONTACT TERMS

In this section, we explicitly present the partial wave contributions of the LO and NLO contact terms of our covariant chiral nuclear force. For simplification, we define

$$\Delta_p = E_p - m, \quad \Delta_{p'} = E_{p'} - m, \quad (9)$$

$$N_p = E_p + m, \quad N_{p'} = E_{p'} + m, \quad (10)$$

$$\Sigma = E_p E_{p'} + m^2, \quad \Gamma = E_p E_{p'} - m^2. \quad (11)$$

The contributions of contact terms to each partial wave then read

$$\begin{aligned} V_{1S0}^{LO} &= 2\pi \left( 2C_1^{1S0} + C_2^{1S0} \frac{\Gamma}{m^2} \right) \\ V_{3P0}^{LO} &= -\frac{2\pi C^{3P0} pp'}{m^2} \\ V_{1P1}^{LO} &= -\frac{2\pi C^{1P1} pp'}{3m^2} \\ V_{3P1}^{LO} &= -\frac{4\pi C^{3P1} pp'}{3m^2} \\ V_{3S1}^{LO} &= C_1^{3S1} \frac{4\pi (7m^2 + 2m(E_p + E_{p'}) - 2E_p E_{p'})}{9m^2} \\ &\quad + C_2^{3S1} \frac{2}{3} \pi \frac{\Gamma}{m^2} \end{aligned} \quad (12)$$

$$\begin{aligned} V_{3D1}^{LO} &= C^{3D1} \frac{8\pi \Delta_p \Delta_{p'}}{9m^2} \\ V_{3S1}^{LO} &= \frac{2\sqrt{2}\pi \Delta_{p'} (6mC_1^{3SD1} + C_2^{3SD1} \Delta_p)}{9m^2} \\ V_{1S0}^{NLO} &= C_1^{1S0} + C_2^{1S0} \frac{(\Delta_p + \Delta_{p'})}{m} \\ &\quad + C_3^{1S0} \frac{(p^2 \Delta_p E_{p'} + p'^2 \Delta_{p'} E_p)}{m^4} \\ &\quad + C_4^{1S0} \frac{p^2 p'^2}{m^2 N_p N_{p'}} + C_5^{1S0} \frac{\Sigma \sqrt{s} (\Delta_p + \Delta_{p'})}{m^4} \\ &\quad + C_6^{1S0} \frac{\sqrt{s} \Delta_p \Delta_{p'}}{m^3} + C_7^{1S0} \frac{(s + \Delta_p E_p + \Delta_{p'} E_{p'})}{m^2} \\ &\quad + C_8^{1S0} \frac{\Gamma s}{m^4} + C_9^{1S0} \frac{(\Delta_p E_p + \Delta_{p'} E_{p'})}{m^2} \\ &\quad + C_{10}^{1S0} \frac{\Delta_p \Delta_{p'} (E_p + E_{p'})}{m^3} + C_{11}^{1S0} \frac{\Delta_p \Delta_{p'} E_p E_{p'}}{m^4} \end{aligned} \quad (13)$$

$$\begin{aligned} V_{3P0}^{NLO} &= C_1^{3P0} \frac{pp'}{m^2} + C_2^{3P0} \frac{pp' (\Delta_p + \Delta_{p'})}{m^3} \\ &\quad + C_3^{3P0} \frac{p^3 p'^3}{m^4 N_p N_{p'}} + C_4^{3P0} \frac{pp' \sqrt{s}}{m^3} \\ &\quad + C_5^{3P0} \frac{pp' \sqrt{s} (\Delta_p + \Delta_{p'})}{m^4} + C_6^{3P0} \frac{pp' s}{m^4} \\ &\quad + C_7^{3P0} \frac{pp' (\Delta_p E_p + \Delta_{p'} E_{p'})}{m^4} \end{aligned} \quad (14)$$



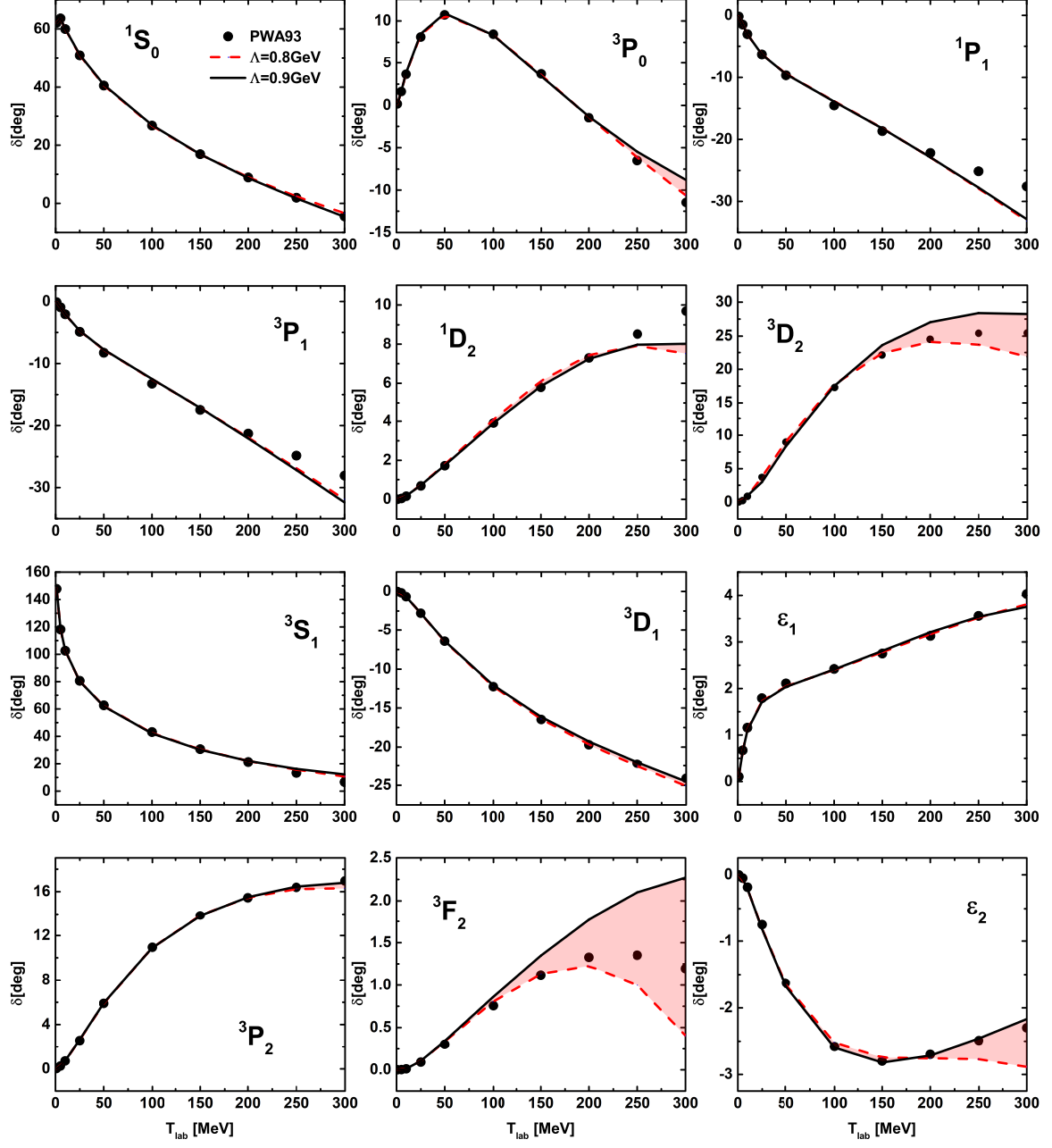


FIG. 4.  $NN$  phase shifts for all the partial waves with  $J \leq 2$  obtained with a variation of the cutoff from 0.8 GeV to 0.9 GeV. The covariant NNLO results obtained with a cutoff of  $\Lambda = 0.8$  GeV and  $\Lambda = 0.9$  GeV are represented with red dashed lines and solid black lines, respectively. The uncertainties due to the cutoff variation are denoted by red shadows.

TABLE V.  $\tilde{\chi}^2 = \sum_i (\delta^i - \delta_{\text{PWA93}}^i)^2$  of different chiral forces for partial waves shown in Fig. 5.

	Total	$^3D_3$	$^1F_3$	$^3F_3$	$^3F_4$	$^3G_3$	$\epsilon_3$	$^1G_4$	$^3G_4$
NNLO	0.98	0.03	0.03	0.21	0.70	0.00	0.01	0.00	0.00
NR-N <sup>3</sup> LO-DR	1.73	0.58	0.73	0.13	0.12	0.00	0.01	0.01	0.15

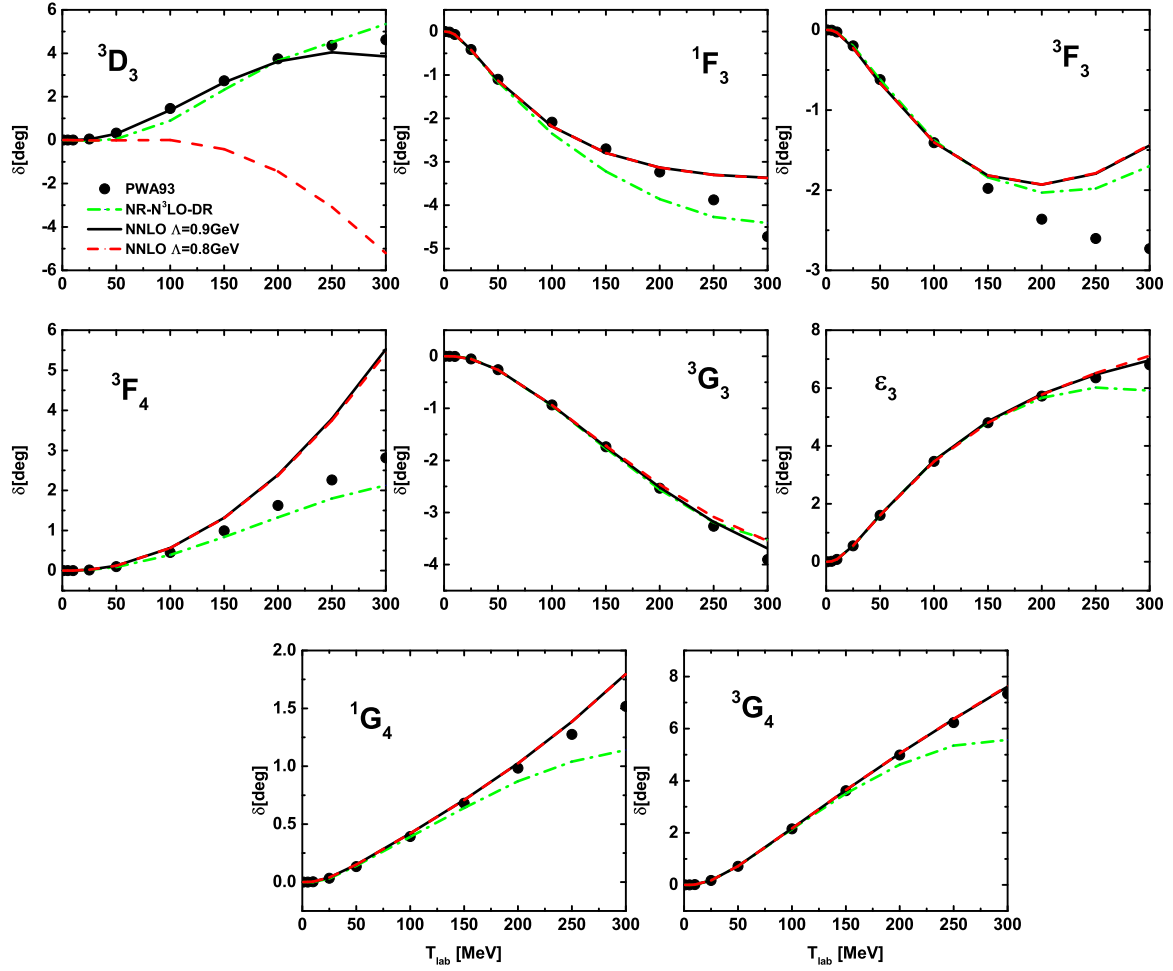


FIG. 5.  $NN$  phase shifts for the peripheral partial waves with  $J \leq 4$  and  $L \leq 4$ . The red dashed lines and black solid lines denote our covariant NNLO results obtained with  $\Lambda = 0.8$  GeV and  $\Lambda = 0.9$  GeV, respectively. For comparison, we also show the NR- $N^3$ LO-DR [11, 51] results denoted by green dash-dotted lines. The black dots denote the PWA93 phase shifts [54].

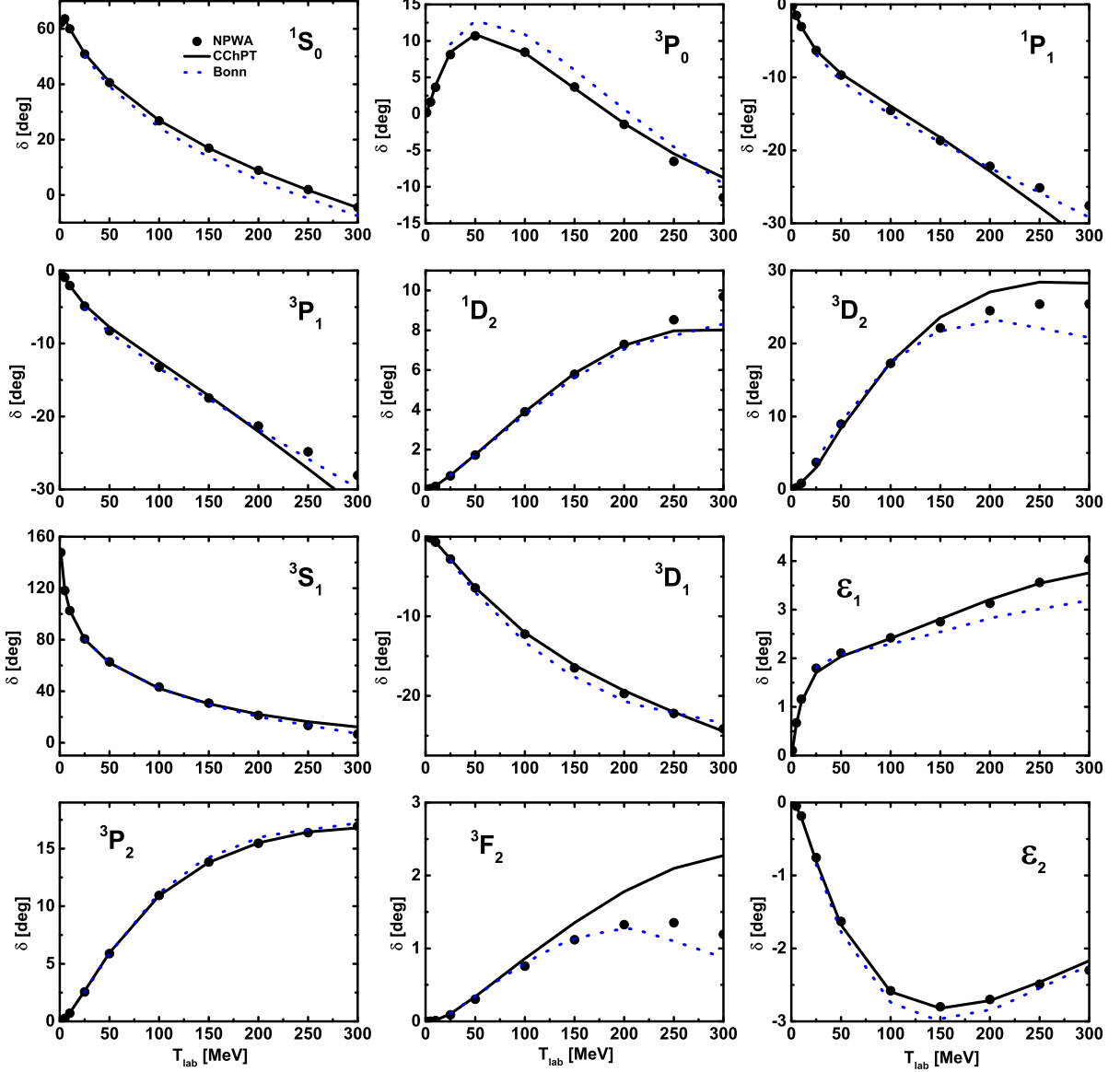


FIG. 6.  $NN$  phase shifts for all the partial waves with  $J \leq 2$  given by the covariant NNLO chiral potential and the Bonn potential [19].

$$\begin{aligned}
 V_{1P1}^{NLO} = & C_1^{1P1} \frac{pp'}{m^2} + C_2^{1P1} \frac{pp'(\Delta_p + \Delta_{p'})}{m^3} \\
 & + C_3^{1P1} \frac{p^3 p'^3}{m^4 N_p N_{p'}} + C_4^{1P1} \frac{pp' \sqrt{s}(E_p + E_{p'})}{m^4} \\
 & + C_5^{1P1} \frac{pp' s}{m^4} + C_6^{1P1} \frac{pp'(\Delta_p E_p + \Delta_{p'} E_{p'})}{m^4}
 \end{aligned} \quad (15)$$

$$\begin{aligned}
 V_{3P1}^{NLO} = & C_1^{3P1} \frac{pp'}{m^2} + C_2^{3P1} \frac{pp'(\Delta_p + \Delta_{p'})}{m^3} \\
 & + C_3^{3P1} \frac{p^3 p'^3}{m^4 N_p N_{p'}} + C_4^{3P1} \frac{pp' \sqrt{s}(E_p + E_{p'})}{m^4} \\
 & + C_5^{3P1} \frac{pp' s}{m^4} + C_6^{3P1} \frac{pp'(\Delta_p E_p + \Delta_{p'} E_{p'})}{m^4}
 \end{aligned} \quad (16)$$

$$\begin{aligned}
 V_{3S1}^{NLO} = & C_1^{3S1} \frac{\Delta_p + \Delta_{p'}}{m} + C_2^{3S1} \frac{p^2 \Delta_p + p'^2 \Delta_{p'}}{m^3} \\
 & + C_3^{3S1} \frac{p^2 p'^2}{m^2 N_p N_{p'}} + C_4^{3S1} \frac{\Delta_p \Delta_{p'} (p^2 + p'^2)}{m^4} \\
 & + C_5^{3S1} \frac{\sqrt{s} (p^2 + p'^2)}{m^3} + C_6^{3S1} \frac{\sqrt{s} \Delta_p \Delta_{p'}}{m^3} \\
 & + C_7^{3S1} \frac{-4m^2 + s + \Delta_p E_p + \Delta_{p'} E_{p'}}{m^2} \\
 & + C_8^{3S1} \frac{s(\Delta_p + \Delta_{p'})}{m^3} + C_9^{3S1} \frac{s \Delta_p \Delta_{p'}}{m^4} \\
 & + C_{10}^{3S1} \frac{\Delta_p E_p + \Delta_{p'} E_{p'}}{m^2} + C_{11}^{3S1} \frac{\Delta_p \Delta_{p'} (E_p + E_{p'})}{m^3} \\
 & + C_{12}^{3S1} \frac{\sqrt{s} \Delta_p \Delta_{p'} (E_p + E_{p'})}{m^4} + C_{13}^{3S1} \frac{\Delta_p \Delta_{p'} E_p E_{p'}}{m^4}
 \end{aligned} \quad (17)$$

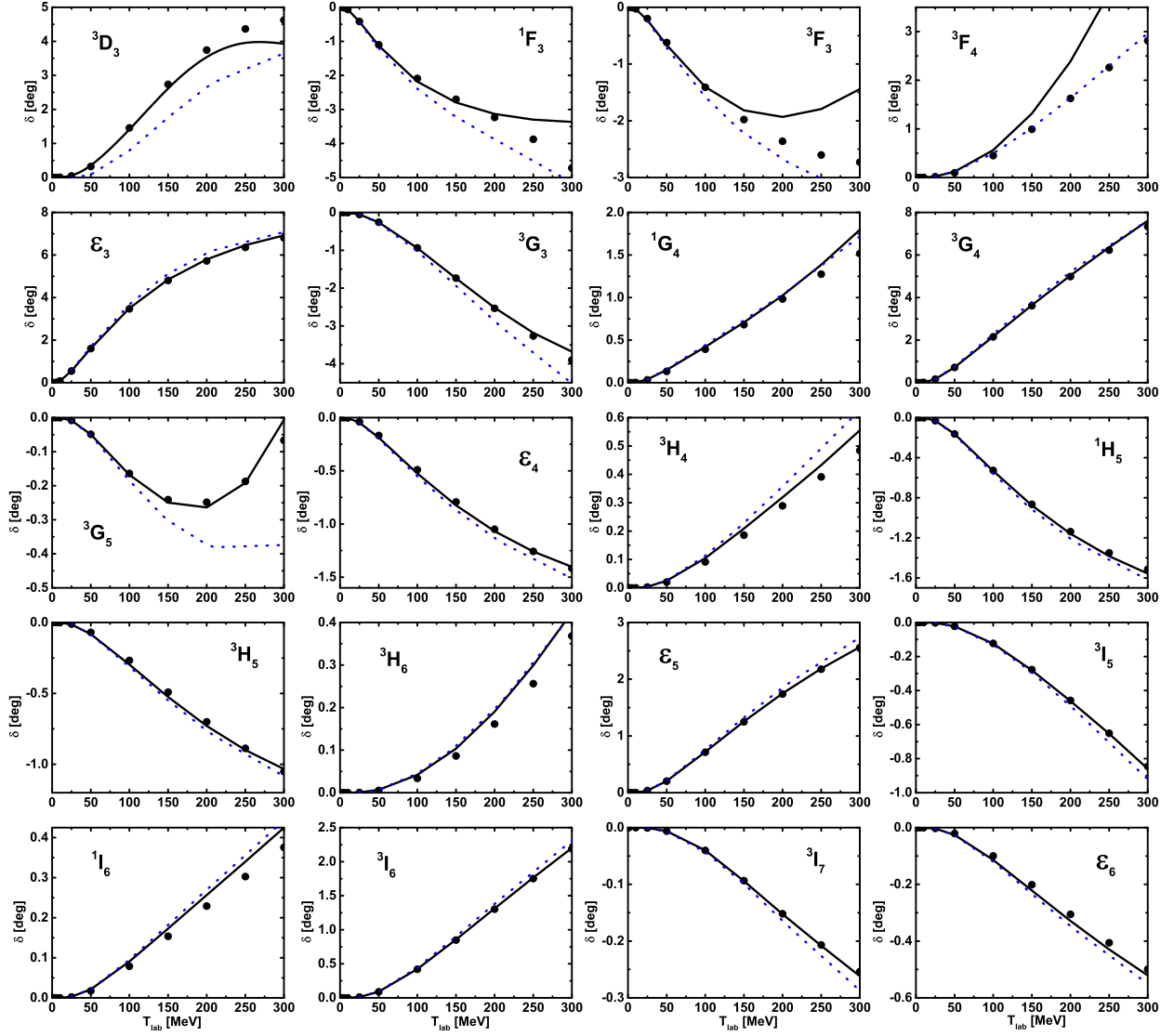


FIG. 7.  $NN$  phase shifts for all the partial waves with  $3 \leq J \leq 7$  given by the covariant NNLO chiral potential and the Bonn potential [19].

$$\begin{aligned}
 V_{3D1}^{NLO} = & C_1^{3D1} \frac{\Delta_p \Delta_{p'}}{m^2} + C_2^{3D1} \frac{\Delta_p \Delta_{p'} (p^2 + p'^2)}{m^4} \\
 & + C_3^{3D1} \frac{\sqrt{s} (p^2 \Delta_{p'} + p'^2 \Delta_p)}{2m^4} + C_4^{3D1} \frac{p^2 p'^2 s}{m^4 N_p N_{p'}} \\
 & + C_5^{3D1} \frac{\Delta_p \Delta_{p'} (E_p + E_{p'})}{m^3} + C_6^{3D1} \frac{\Delta_p \Delta_{p'} E_p E_{p'}}{m^4}
 \end{aligned} \quad (18)$$

$$\begin{aligned}
 V_{3SD1}^{NLO} = & C_1^{3SD1} \frac{\sqrt{2} \Delta_{p'}}{9m} + C_2^{3SD1} \frac{\sqrt{2} \Delta_{p'}^2 N_{p'}}{9m^3} \\
 & + C_3^{3SD1} \frac{\sqrt{2} \Delta_p \Delta_{p'}}{9m^2} + C_4^{3SD1} \frac{\sqrt{2} \Delta_p \Delta_{p'} (p^2 + p'^2)}{9m^4} \\
 & + C_5^{3SD1} \frac{\sqrt{2} s \Delta_{p'} (\sqrt{s} + N_{p'})}{9m^3} \\
 & + C_6^{3SD1} \frac{\sqrt{2} s \Delta_p \Delta_{p'}}{9m^3} + C_7^{3SD1} \frac{\sqrt{2} s \Delta_{p'}}{9m^3} \\
 & + C_8^{3SD1} \frac{\sqrt{2} s \Delta_p \Delta_{p'}}{9m^4} + C_9^{3SD1} \frac{\sqrt{2} \Delta_{p'} E_{p'}}{9m^2} \\
 & + C_{10}^{3SD1} \frac{\sqrt{2} \Delta_p \Delta_{p'} E_{p'}}{9m^3} + C_{11}^{3SD1} \frac{\sqrt{2} s \Delta_p \Delta_{p'} (E_p + E_{p'})}{9m^4} \\
 & + C_{12}^{3SD1} \frac{\sqrt{2} \Delta_p \Delta_{p'} E_p}{9m^3} \\
 & + C_{13}^{3SD1} \frac{\sqrt{2} \Delta_p \Delta_{p'} E_p E_{p'}}{9m^4}
 \end{aligned} \quad (19)$$



$$\begin{aligned}
V_{1D2}^{NLO} &= \frac{C^{1D2} p^2 p'^2}{m^4} \\
V_{3D2}^{NLO} &= \frac{C^{3D2} p^2 p'^2}{m^4} \\
V_{3P2}^{NLO} &= C_1^{3P2} \frac{pp'}{m^2} + C_2^{3P2} \frac{pp'(\Delta_p + \Delta_{p'})}{m^3} \\
&\quad + C_3^{3P2} \frac{p^3 p'^3}{m^4 N_p N_{p'}} \\
V_{3F2}^{NLO} &= C_3^{3F2} \frac{p^3 p'^3}{m^4 N_p N_{p'}} \\
V_{3P2-3F2}^{NLO} &= C_1^{3PF2} \frac{2\sqrt{\frac{2}{3}}}{25} \frac{pp'^3}{m^3 N_{p'}} \\
&\quad + C_2^{3PF2} \frac{\sqrt{\frac{2}{3}} p^3 p'^3}{25 m^4 N_p N_{p'}}
\end{aligned} \tag{20}$$

Note that a factor of  $\pi$  is omitted in Eqs. (13-20). The partial wave combinations in terms of the LECs appear in the covariant Lagrangians are given as follows.

$$\begin{aligned}
C_1^{1S0} &= O_1 + O_2 + 3O_3 - 6O_4 \\
C_2^{1S0} &= O_1 + 4(O_2 + O_3 - 3O_4) \\
C^{3P0} &= O_1 - 4(O_2 + O_3 + 3O_4) \\
C^{1P1} &= O_1 + 4O_4 \\
C^{3P1} &= O_1 - 2O_2 + 2O_3 \\
C_1^{3S1} &= O_1 + O_2 - O_3 + 2O_4 \\
C_2^{3S1} &= 3O_1 + 4O_2 - 4O_3 - 4O_4 \\
C^{3D1} &= O_1 + O_2 - O_3 + 2O_4 \\
C_1^{3SD1} &= O_1 + O_2 - O_3 + 2O_4 \\
C_1^{3SD1} &= O_1 + 4O_2 - 4O_3 - 4O_4
\end{aligned} \tag{21}$$

$$\begin{aligned}
C_1^{1S0} &= -4O_{14} - 4O_{15} - 12O_{16} + 24O_{17} \\
C_2^{1S0} &= -O_{10} - O_{11} - 3O_{12} + 6O_{13} - O_{14} \\
&\quad - 7O_{15} - 5O_{16} + 18O_{17} + 2O_5 + O_6 - 2O_7 + 2O_9 \\
C_3^{1S0} &= -\frac{O_{10}}{2} - 2O_{11} - 2O_{12} + 6O_{13} + \frac{O_{14}}{2} + 2O_{15} \\
&\quad + 2O_{16} - 6O_{17} + \frac{O_6}{2} - \frac{3O_7}{2} + \frac{3O_9}{2} \\
C_4^{1S0} &= -\frac{4O_{10}}{3} - 4O_{11} - 4O_{12} + \frac{32O_{13}}{3} - \frac{4O_{14}}{3} - 4O_{15} \\
&\quad - 4O_{16} + \frac{32O_{17}}{3} + 2O_5 + 2O_6 - \frac{10O_7}{3} + \frac{4O_8}{3} + \frac{8O_9}{3} \\
C_5^{1S0} &= 2O_6 - 4O_7 + 2O_8 \\
C_6^{1S0} &= 4O_6 - 8O_7 + 4O_8 \\
C_7^{1S0} &= O_{14} + O_{15} + 3O_{16} - 6O_{17} \\
C_8^{1S0} &= \frac{O_{14}}{2} + 2O_{15} + 2O_{16} - 6O_{17} + 2O_6 - 6O_7 \\
C_9^{1S0} &= -O_{10} - O_{11} - 3O_{12} + 6O_{13} + O_6 - 2O_7 + 2O_9 \\
C_{10}^{1S0} &= -\frac{5O_{10}}{6} - 2O_{11} - 2O_{12} + \frac{14O_{13}}{3} + \frac{O_{14}}{6} + 2O_{15} \\
&\quad + 2O_{16} - \frac{22O_{17}}{3} + \frac{3O_6}{2} - \frac{11O_7}{6} + \frac{4O_8}{3} + \frac{7O_9}{6} \\
C_{11}^{1S0} &= -\frac{O_{10}}{3} - \frac{4O_{13}}{3} - \frac{O_{14}}{3} - \frac{4O_{17}}{3} + O_6 - \frac{O_7}{3} \\
&\quad + \frac{4O_8}{3} - \frac{O_9}{3}
\end{aligned} \tag{22}$$

$$\begin{aligned}
C_1^{3P0} &= \frac{2O_{10}}{3} + \frac{2O_{11}}{3} - \frac{2O_{12}}{3} + \frac{4O_{13}}{3} + \frac{8O_{14}}{3} - \frac{22O_{15}}{3} \\
&\quad - \frac{26O_{16}}{3} - \frac{68O_{17}}{3} - 2O_5 + 2O_6 + \frac{8O_7}{3} - \frac{8O_8}{3} + \frac{8O_9}{3} \\
C_2^{3P0} &= \frac{5O_{10}}{6} - 2O_{11} - 2O_{12} - \frac{14O_{13}}{3} - \frac{O_{14}}{6} + 2O_{15} \\
&\quad + 2O_{16} + \frac{22O_{17}}{3} + \frac{3O_6}{2} + \frac{11O_7}{6} - \frac{4O_8}{3} - \frac{7O_9}{6} \\
C_3^{3P0} &= \frac{O_{10}}{3} + \frac{4O_{13}}{3} + \frac{O_{14}}{3} + \frac{4O_{17}}{3} + O_6 + \frac{O_7}{3} \\
&\quad - \frac{4O_8}{3} + \frac{O_9}{3} \\
C_4^{3P0} &= 4O_6 + 8O_7 - 4O_8 \\
C_5^{3P0} &= 2O_6 + 4O_7 - 2O_8 \\
C_6^{3P0} &= -\frac{O_{14}}{2} + 2O_{15} + 2O_{16} + 6O_{17} + 2O_6 + 6O_7 \\
C_7^{3P0} &= \frac{O_{10}}{2} - 2O_{11} - 2O_{12} - 6O_{13} - \frac{O_{14}}{2} + 2O_{15} \\
&\quad + 2O_{16} + 6O_{17} + \frac{O_6}{2} + \frac{3O_7}{2} - \frac{3O_9}{2}
\end{aligned} \tag{23}$$

$$\begin{aligned}
C_1^{1P1} &= \frac{2O_{10}}{3} + \frac{2O_{11}}{3} + 2O_{12} - 4O_{13} + \frac{4O_{14}}{3} + \frac{2O_{15}}{3} \\
&\quad + 2O_{16} - \frac{4O_{17}}{3} - \frac{2O_5}{3} + \frac{2O_6}{3} - \frac{4O_7}{3} - \frac{4O_9}{3} \\
C_2^{1P1} &= \frac{O_{10}}{2} + \frac{4O_{11}}{3} + \frac{4O_{12}}{3} - \frac{10O_{13}}{3} + \frac{O_{14}}{6} + \frac{4O_{15}}{3} \\
&\quad + \frac{4O_{16}}{3} - \frac{14O_{17}}{3} + \frac{O_6}{2} - \frac{7O_7}{6} - \frac{5O_9}{6} \\
C_3^{1P1} &= \frac{O_{10}}{3} + \frac{4O_{11}}{3} + \frac{4O_{12}}{3} - 4O_{13} + \frac{O_{14}}{3} + \frac{4O_{15}}{3} \\
&\quad + \frac{4O_{16}}{3} - 4O_{17} + \frac{O_6}{3} - O_7 - O_9 \\
C_4^{1P1} &= \frac{2O_6}{3} - \frac{4O_7}{3} - \frac{2O_8}{3} \\
C_5^{1P1} &= -\frac{O_{14}}{6} - \frac{2O_{17}}{3} + \frac{2O_6}{3} - \frac{2O_7}{3} \\
C_6^{1P1} &= \frac{O_{10}}{6} + \frac{2O_{13}}{3} - \frac{O_{14}}{6} - \frac{2O_{17}}{3} + \frac{O_6}{6} - \frac{O_7}{6} + \frac{O_9}{6}
\end{aligned} \tag{24}$$

$$\begin{aligned}
C_1^{3P1} &= \frac{2O_{10}}{3} + \frac{2O_{11}}{3} - \frac{2O_{12}}{3} + \frac{4O_{13}}{3} + 2O_{14} - 2O_{15} \\
&\quad + 2O_{16} + \frac{4O_{17}}{3} + \frac{4O_5}{3} - \frac{4O_6}{3} - \frac{2O_7}{3} - \frac{4O_8}{3} - \frac{2O_9}{3} \\
C_2^{3P1} &= \frac{2O_{10}}{3} + \frac{4O_{15}}{3} - \frac{4O_{16}}{3} - O_6 - \frac{2O_7}{3} \\
&\quad - \frac{2O_8}{3} - \frac{4O_9}{3} \\
C_3^{3P1} &= \frac{O_{10}}{3} + \frac{2O_{11}}{3} - \frac{2O_{12}}{3} + \frac{O_{14}}{3} + \frac{2O_{15}}{3} - \frac{2O_{16}}{3} \\
&\quad - \frac{2O_6}{3} - O_7 - \frac{2O_8}{3} - O_9 \\
C_4^{3P1} &= -\frac{4O_6}{3} - \frac{4O_8}{3} \\
C_5^{3P1} &= -\frac{O_{14}}{3} + \frac{2O_{15}}{3} - \frac{2O_{16}}{3} - \frac{4O_6}{3} + \frac{4O_7}{3} \\
C_6^{3P1} &= \frac{O_{10}}{3} - \frac{2O_{11}}{3} + \frac{2O_{12}}{3} - \frac{O_{14}}{3} + \frac{2O_{15}}{3} - \frac{2O_{16}}{3} \\
&\quad - \frac{O_6}{3} + \frac{O_7}{3} - \frac{O_9}{3}
\end{aligned} \tag{25}$$

$$\begin{aligned}
C_1^{3S1} &= -O_{10} - O_{11} + O_{12} - 2O_{13} - O_{14} - \frac{5O_{15}}{3} \\
&\quad + \frac{5O_{16}}{3} - \frac{2O_{17}}{3} - \frac{2O_5}{3} - \frac{O_6}{3} + \frac{2O_7}{3} - \frac{2O_9}{3} \\
C_2^{3S1} &= -\frac{O_{10}}{2} - \frac{2O_{11}}{3} + \frac{2O_{12}}{3} - \frac{2O_{13}}{3} + \frac{O_{14}}{2} + \frac{2O_{15}}{3} \\
&\quad - \frac{2O_{16}}{3} + \frac{2O_{17}}{3} - \frac{O_6}{6} - \frac{O_7}{6} + \frac{O_9}{6} \\
C_3^{3S1} &= -\frac{4O_{10}}{3} - \frac{4O_{11}}{9} + \frac{4O_{12}}{3} - \frac{4O_{14}}{9} + \frac{4O_{15}}{9} + \frac{4O_{16}}{9} \\
&\quad + \frac{16O_{17}}{9} - \frac{2O_5}{3} - \frac{2O_6}{3} + \frac{14O_7}{9} + \frac{4O_8}{9} + \frac{4O_9}{9} \\
C_4^{3S1} &= -\frac{5O_{10}}{18} - \frac{4O_{11}}{9} + \frac{4O_{12}}{9} - \frac{2O_{13}}{9} + \frac{5O_{14}}{18} + \frac{4O_{15}}{9} \\
&\quad - \frac{4O_{16}}{9} + \frac{2O_{17}}{9} - \frac{O_6}{6} - \frac{O_7}{6} + \frac{O_9}{6} \\
C_5^{3S1} &= -\frac{2O_6}{3} + \frac{4O_7}{3} + 2O_8 \\
C_6^{3S1} &= -\frac{4O_6}{3} + \frac{8O_7}{9} + \frac{20O_8}{9} \\
C_7^{3S1} &= O_{14} + O_{15} - O_{16} + 2O_{17} \\
C_8^{3S1} &= \frac{O_{14}}{2} + \frac{2O_{15}}{3} - \frac{2O_{16}}{3} + \frac{2O_{17}}{3} - \frac{2O_6}{3} - \frac{2O_7}{3} \\
C_9^{3S1} &= \frac{5O_{14}}{18} + \frac{4O_{15}}{9} - \frac{4O_{16}}{9} + \frac{2O_{17}}{9} - \frac{2O_6}{3} - \frac{2O_7}{3} \\
C_{10}^{3S1} &= -O_{10} - O_{11} + O_{12} - 2O_{13} - \frac{O_6}{3} + \frac{2O_7}{3} - \frac{2O_9}{3} \\
C_{11}^{3S1} &= -\frac{5O_{10}}{6} + \frac{2O_{11}}{9} + \frac{2O_{12}}{3} + \frac{2O_{13}}{3} + \frac{O_{14}}{6} + \frac{14O_{15}}{9} \\
&\quad - \frac{2O_{16}}{3} + 2O_{17} - \frac{O_6}{2} + \frac{23O_7}{18} + \frac{4O_8}{9} + \frac{13O_9}{18} \\
C_{12}^{3S1} &= -\frac{2O_6}{3} + \frac{4O_7}{9} + \frac{10O_8}{9} \\
C_{13}^{3S1} &= -\frac{O_{10}}{3} + \frac{8O_{11}}{9} + \frac{4O_{13}}{3} - \frac{O_{14}}{3} + \frac{8O_{15}}{9} + \frac{4O_{17}}{3} \\
&\quad - \frac{O_6}{3} + O_7 + \frac{4O_8}{9} + O_9
\end{aligned} \tag{26}$$

$$\begin{aligned}
C_1^{3D1} &= -\frac{O_{10}}{3} + \frac{10O_{11}}{9} + \frac{2O_{12}}{3} + \frac{8O_{13}}{3} - \frac{11O_{14}}{9} \\
&\quad + \frac{2O_{15}}{9} + \frac{14O_{16}}{9} + \frac{8O_{17}}{9} + \frac{O_7}{9} + \frac{2O_8}{9} + \frac{17O_9}{9} \\
C_2^{3D1} &= -\frac{2O_{10}}{9} - \frac{2O_{11}}{9} + \frac{2O_{12}}{9} - \frac{4O_{13}}{9} + \frac{2O_{14}}{9} + \frac{2O_{15}}{9} \\
&\quad - \frac{2O_{16}}{9} + \frac{4O_{17}}{9} \\
C_3^{3D1} &= \frac{16O_7}{9} + \frac{16O_8}{9} \\
C_4^{3D1} &= \frac{2O_{14}}{9} + \frac{2O_{15}}{9} - \frac{2O_{16}}{9} + \frac{4O_{17}}{9} \\
C_5^{3D1} &= -\frac{O_{10}}{3} + \frac{10O_{11}}{9} + \frac{2O_{12}}{3} + \frac{8O_{13}}{3} - \frac{O_{14}}{3} + \frac{10O_{15}}{9} \\
&\quad + \frac{2O_{16}}{3} + \frac{8O_{17}}{3} + \frac{5O_7}{9} + \frac{2O_8}{9} + \frac{13O_9}{9} \\
C_6^{3D1} &= -\frac{O_{10}}{3} + \frac{10O_{11}}{9} + \frac{2O_{12}}{3} + \frac{8O_{13}}{3} - \frac{O_{14}}{3} + \frac{10O_{15}}{9} \\
&\quad + \frac{2O_{16}}{3} + \frac{8O_{17}}{3} + O_7 + \frac{2O_8}{9} + O_9
\end{aligned} \tag{27}$$

$$\begin{aligned}
C_1^{3SD1} &= -12O_{15} + 12O_{16} + 24O_{17} - 12O_5 \\
&\quad - 6O_6 - 6O_7 + 6O_9 \\
C_2^{3SD1} &= -3O_{11} + 3O_{12} + 6O_{13} + 3O_{15} - 3O_{16} \\
&\quad - 6O_{17} - 3O_6 - 3O_7 + 3O_9 \\
C_3^{3SD1} &= -5O_{11} - 3O_{12} - 6O_{13} - 2O_{14} - 7O_{15} \\
&\quad - O_{16} - 10O_{17} - 6O_5 - 6O_6 - 5O_7 + 2O_8 + 5O_9 \\
C_4^{3SD1} &= -\frac{O_{10}}{2} - 2O_{11} + 2O_{12} + 2O_{13} + \frac{O_{14}}{2} + 2O_{15} \\
&\quad - 2O_{16} - 2O_{17} - \frac{3O_6}{2} - \frac{3O_7}{2} + \frac{3O_9}{2} \\
C_5^{3SD1} &= -12O_6 - 12O_7 \\
C_6^{3SD1} &= -12O_6 - 8O_7 + 4O_8 \\
C_7^{3SD1} &= 3O_{15} - 3O_{16} - 6O_{17} \\
C_8^{3SD1} &= \frac{O_{14}}{2} + 2O_{15} - 2O_{16} - 2O_{17} - 6O_6 - 6O_7 \\
C_9^{3SD1} &= -6O_6 - 6O_7 + 6O_9 \\
C_{10}^{3SD1} &= -2O_{11} - 6O_{12} - 12O_{13} - 2O_{15} - 6O_{16} \\
&\quad - 12O_{17} - 6O_6 - 4O_7 + 2O_8 + 4O_9 \\
C_{11}^{3SD1} &= -6O_6 - 4O_7 + 2O_8 \\
C_{12}^{3SD1} &= -5O_{11} - 3O_{12} - 6O_{13} + O_{15} - 9O_{16} \\
&\quad - 18O_{17} - 3O_6 - O_7 + 2O_8 + O_9 \\
C_{13}^{3SD1} &= -2O_{11} - 6O_{12} - 12O_{13} - 2O_{15} - 6O_{16} \\
&\quad - 12O_{17} - 3O_6 + 2O_8
\end{aligned} \tag{28}$$

$$\begin{aligned}
C^{1D2} &= -\frac{2O_{10}}{15} - \frac{8O_{13}}{15} - \frac{2O_{14}}{15} - \frac{8O_{17}}{15} - \frac{2O_7}{15} \\
&\quad - \frac{4O_8}{15} - \frac{2O_9}{15} \\
C^{3D2} &= -\frac{O_{10}}{5} + \frac{2O_{11}}{5} - \frac{2O_{12}}{5} - \frac{O_{14}}{5} + \frac{2O_{15}}{5} - \frac{2O_{16}}{5} \\
&\quad - \frac{O_7}{5} - \frac{2O_8}{5} - \frac{O_9}{5} \\
C_1^{3P2} &= \frac{2O_{10}}{75} + \frac{2O_{11}}{75} - \frac{2O_{12}}{75} + \frac{4O_{13}}{75} + \frac{2O_{14}}{75} + \frac{2O_{15}}{75} \\
&\quad - \frac{2O_{16}}{75} + \frac{4O_{17}}{75} + \frac{2O_7}{75} + \frac{4O_8}{75} + \frac{2O_9}{75} \\
C_2^{3P2} &= \frac{O_{10}}{75} + \frac{2O_{11}}{25} - \frac{2O_{12}}{25} - \frac{8O_{13}}{75} + \frac{O_{14}}{75} + \frac{2O_{15}}{25} \\
&\quad - \frac{2O_{16}}{25} - \frac{8O_{17}}{75} + \frac{O_7}{75} + \frac{2O_8}{75} + \frac{O_9}{75} \\
C_3^{3P2} &= \frac{13O_{10}}{75} + \frac{6O_{11}}{25} - \frac{6O_{12}}{25} + \frac{16O_{13}}{75} + \frac{13O_{14}}{75} \\
&\quad + \frac{6O_{15}}{25} - \frac{6O_{16}}{25} + \frac{16O_{17}}{75} + \frac{13O_7}{75} + \frac{26O_8}{75} + \frac{13O_9}{75} \\
C^{3F2} &= \frac{4O_{10}}{25} + \frac{4O_{11}}{25} - \frac{4O_{12}}{25} + \frac{8O_{13}}{25} + \frac{4O_{14}}{25} + \frac{4O_{15}}{25} \\
&\quad - \frac{4O_{16}}{25} + \frac{8O_{17}}{25} + \frac{4O_7}{25} + \frac{8O_8}{25} + \frac{4O_9}{25} \\
C_1^{3PF2} &= 5O_{11} - 5O_{12} - 10O_{13} + 5O_{15} - 5O_{16} - 10O_{17} \\
C_2^{3PF2} &= O_{10} + 6O_{11} - 6O_{12} - 8O_{13} + O_{14} + 6O_{15} \\
&\quad - 6O_{16} - 8O_{17} + O_7 + 2O_8 + O_9
\end{aligned} \tag{29}$$